Empirical Channel Stationarity in Urban Environments

Andreas Gehring[1], Martin Steinbauer[1], Ingo Gaspard[2] and Michael Grigat[2]
[1] Institut für Nachrichtentechnik und Hochfrequenztechnik (E389),
Gußhausstraße 25-29, A-1040 Wien, Austria,
[2] T-NOVA Deutsche Telekom Innovationsgesellschaft mbH
{gehring@iue,steinbauer@nt}.tuwien.ac.at

Abstract— **Large-scale channel modeling requires knowledge of the rate and amount of variations in the small-scale statistics. We introduce the concept of local stationarity regions to segment radio channel measurements into parts that are stationary on a small-scale basis. By imposing a threshold on the correlation coefficient between consecutive power delay profiles, we define the *local region of stationarity* (LRS) as the set of positions of the mobile station where this correlation coefficient exceeds the threshold. A correlation threshold of 0.5 gives a good compromise between identifiability of stationarity regions and approximation with a constant PDP within. Evaluation of measurement data for urban, suburban and factory environments show that the LRS length grows with the base station height as soon as it exceeds the average building height. The median size of these regions was approximately 5m in the investigated urban environments. We compare the measurement data to standard probability density functions and find that the LRS length can be modeled by a lognormal distribution.**

I. Introduction

SEVERAL propagation effects have been identified for the mobile radio channel in the past [1], [2]. From the different time-scales, usually a three-stage structure is envisaged: (i) the *small-scale fading* results from multipath interference and is thus changing on a wavelength scale; (ii) the *large-scale fading* is due to shadowing from surrounding obstacles and can be extracted from the received power by averaging over 10...40 wavelengths; and finally is (iii) the *pathloss* which has to be evaluated over a region of about 100 wavelengths.

The three-stage hierarchy in propagation effects is the key for channel simulators based upon the WSSUS (Wide Sense Stationary Uncorrelated Scatterers) principle [3], [4]. While many simulators of this kind only reproduce the small-scale fading, some also include large-scale variations by means of transitions between WSSUS channel states, each representing a certain small-scale region [5], [6], [7].

For the sake of accuracy, switching between channel states should be made as often as possible. However, in higher complexity channel models like *geometry based* models [8] generation of a new small-scale channel state is usually computationally expensive. Therefore, channel updates should remain seldom. In other words, to reflect the real-world channel behavior, channel updates in a simulator should be made in accordance with the rate of measured (large-scale) channel fluctuations but not at a higher rate.

Measurement data is usually recorded on a run basis. This means that one measurement run comprising many subsequent channel impulse responses is stored in one file while the mobile station is moving on a prescribed route. This route is selected according to a realistic user scenario. Therefore, all propagation effects mentioned above are contained in the measurement data. Then, however, these data must not be used directly to compute small-scale parameters like Doppler spectra. A *segmentation* of all the data into *local regions of stationarity* (LRS) is needed in advance. Only after the segmentation, the small-scale parameters can be computed rigorously for each LRS and become physically meaningful.

The changing from one small-scale channel state to another is often referred to as *non-stationary* behavior. While popular common models [9] already include non-stationarity, parameters for the occurrence of these non-stationarities are difficult to obtain. Why are non-stationarities such a problem? 3G systems will employ rake receivers and due to their need for an acquisition phase, they are extremely sensitive to sudden changes of the channel response. In the worst case, the fingers are completely mistuned after the instationarity in the channel and the acquisition has to be started from scratch. Therefore, realistic simulations of Rake receivers need the channel stationarity to be modeled accurately. Since the output of different fingers are input to a suitable combiner, it is not sufficient to just look on the large-scale behavior of the narrowband fieldstrength where all multipath components (MPCs) occur aggregated by random phases[1]. Obviously, realistic simulation of

[1] A. Gehring is now with the Institut für Mikroelektronik (E360), Gusshausstrasse 27-29, A-1040 Wien, Austria

[1] For example, it might be that one dominant MPC vanishes while another rises at the same time. The narrowband power might remain nearly constant although the new channel im-

wideband systems incorporating rake receivers needs to handle non-stationarities. One concept is proposed here: local stationarity regions.

The outline of the paper is as follows. First, we use the correlation coefficient to define the Local Region of Stationarity. We continue with a description of the different measurement environments, followed by measurement results. We compare the derived LRS lengths for different correlation threshold values and environments. Then, we compare the results to different distribution functions. Finally, we draw some conclusions.

II. The Local Region of Stationarity

Measurement campaigns usually yield a series of complex impulse responses $h(t_i, \tau)$, where t_i is the absolute time of observation for the i-th snapshot and τ the propagation delay. Assuming a constant speed of the mobile throughout the measurement run, the absolute time t can be related to the traveled distance via $x = v \cdot t$. If this assumption is not fulfilled, the same definition applies with all absolute time variables $(t, \Delta t)$ replaced by corresponding distance measures $(x, \Delta x)$. Regardless of the computation or sounding method, the LRS is always given as a distance measure which corresponds better to its physical background. This also allows one to simulate variable mobile speeds.

In the sequel, we use the term *stationary* not in its mathematical-statistical meaning but to express that the small-scale behavior of the channel remains unchanged. This corresponds to scatterers remaining observably constant in space. A *nonstationarity* occurs as soon as the scattering ensemble has changed and thus the multipath interference pattern has become different.

For the definition of local stationarity regions, we start with the instantaneous *power delay profile*, $P_h(t_i, \tau) = |h(t_i, \tau)|^2$, and average over several of them to eliminate fast fading

$$\overline{P_h(t_i, \tau)} = \frac{1}{N} \sum_{i}^{i+N-1} |h(t_i, \tau)|^2. \qquad (1)$$

The number N of power delay profiles to be averaged is chosen to satisfy

$$N = \left\lceil \frac{T_{ss}}{\Delta t} \right\rceil \qquad (2)$$

with T_{ss} denoting the small-scale averaging duration

$$T_{ss} = \frac{15\lambda}{v}, \qquad (3)$$

and Δt being the repetition period at which consecutive channel snapshots are recorded. The mobile's speed enters via v, and the averaging interval is set to 15 wavelengths λ which is a compromise based on the studied effect on the correlation coefficient between averaged PDPs. This *sliding window* averaging procedure is depicted in Fig. 1 for N=3.

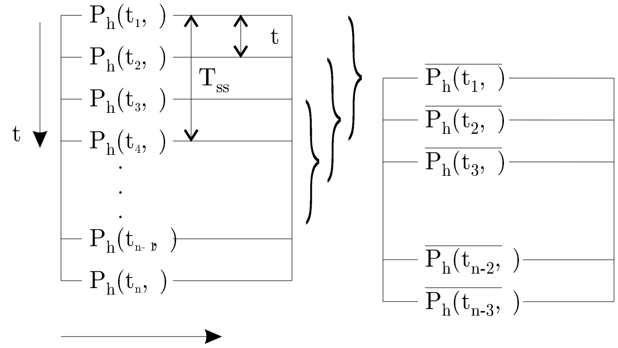

Fig. 1. Sliding window averaging of instantaneous power delay profiles.

The (temporal) *correlation coefficient* between two averaged PDPs can now be computed as

$$c(t_i, \Delta t) = \frac{\int \overline{P_h(t_i, \tau)} \cdot \overline{P_h(t_i + \Delta t, \tau)} d\tau}{\max \left\{ \int \overline{P_h(t_i, \tau)}^2 d\tau, \int \overline{P_h(t_i + \Delta t, \tau)}^2 d\tau \right\}} \qquad (4)$$

We define the *local region of stationarity* (LRS) as the geographical region where, starting from its maximum value, the correlation coefficient does not undergo a certain threshold c_{th}. The (spatial) LRS length then evaluates to

$$d_{LRS}(t_i) = \max \left\{ \Delta x \left|_{c(t_i, \Delta t) \geq c_{th}} \right. \right\} \qquad (5)$$

$$\Delta x = v \cdot \Delta t \qquad (6)$$

Figure 2 gives a physical example of a non-stationarity and how it is detected by our segmentation procedure. As long as the channel does not change severely (from a mobile station/user equipment point of view), the measured power delay profiles are quite similar, resulting in a high correlation coefficient. As soon as the mobile station turns

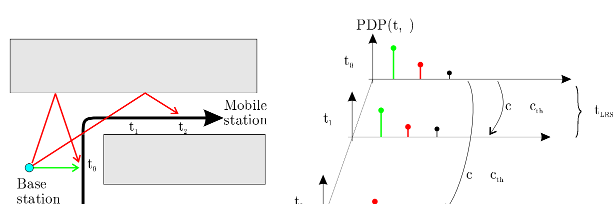

Fig. 2. Non-stationarity detection via segmentation into local stationarity regions.

pulse response could be even orthogonal to the old one!

around the corner, the line-of-sight (LOS) path vanishes and other paths become stronger. The measured PDP behind the corner is completely different than before, resulting in a low correlation coefficient.

A. *Large-scale error norm*

To quantify the error made by replacing the original stream of PDPs $\underline{P_h(t_i,\tau)}$ with a series of LRS-specific (equal) PDPs $\overline{P_h(t_i,\tau)}$, we introduce the relative error ϵ between any two PDPs,

$$\epsilon(t_i,\Delta t) = \frac{\int \left|\overline{P_h(t_i,\tau)} - \overline{P_h(t_i+\Delta t,\tau)}\right| d\tau}{\max\left\{\int \overline{P_h(t_i,\tau)}d\tau, \int \overline{P_h(t_i+\Delta t,\tau)}d\tau\right\}} \tag{7}$$

This expression gives the relative difference between the averaged power delay profiles at the times t_i and $t_i + \Delta t$, normalized to the larger one. The higher ϵ, the higher is the difference between the measured PDP.

III. Measurement Evaluation

To test the hypothesis of local stationarity regions describing small-scale channel states that can be used to replace the raw measurement data stream, we applied it on typical measurement results. Before turning to the resulting LRS lengths, we describe the measurement setup and the investigated environments.

A. *Measurement Setup*

Measurements have been performed by T-NOVA in several urban environments. The measurement frequency was around 1.8 GHz with a sampling rate of 10 MHz. An impulse response was recorded every 24 ms. The speed of the mobile station varied from 5 to 15 km/h and remained constant during the measurement. Three different environments have been investigated: Dresden-Prohlis (Fig. 3), Mannheim City (Fig. 4), and Frankfurt station. **Dresden** can be classified as typical *suburban* environment. The base station was mounted at location BS1 at a height of 4.5 meters. The average building height was 20 meters. In **Frankfurt**, measurements have been performed in a railway station. The base station was located at 2.2 meters height in the station terminal and the receiver was moved along the platforms. This environment resembles a *factory* environment with main obstacles of 4 meters height. In **Mannheim**, the average building height was again 20 meters, but measurements have been performed with three different base station heights, namely 14.8m, 19m and 26.7m. With its rectangular street grid and building block structure, this environment falls into the category *(bad) urban*.

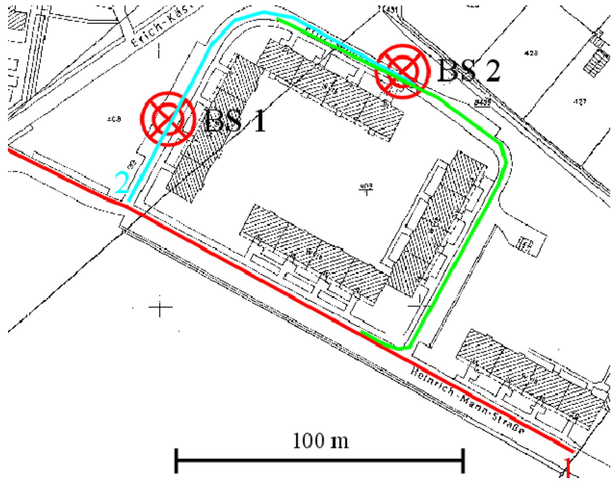

Fig. 3. Dresden-Prohlis measurement scenario.

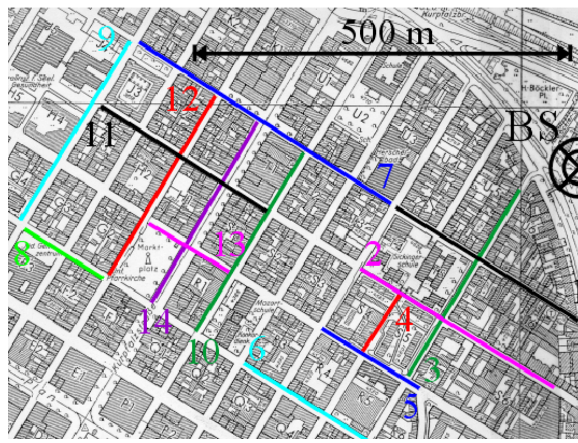

Fig. 4. Mannheim City measurement scenario.

B. *Measurement Results*

Figure 5 shows the correlation coefficient for Dresden-Prohlis. For each position of the mobile station, the correlation coefficient to each other point in the measurement run is given. Obvious is the symmetric structure which is typical for any autocorrelation function. It can be seen that after 40 meters and 115 meters, the channel changes significantly. The corresponding averaged PDP for this environment is shown in Fig. 6. What happens?

It can easily be seen how the channel changes when the mobile station leaves the first block of houses at 40m and turns around the corner at 115m. From the correlation plot, we see that the region where the correlation coefficient c is higher than 0.9 is very small, only some meters. Therefore we used a correlation threshold value of $c_t = 0.5$ to get higher and more distinguishable values of the LRS length. The corresponding LRS length can be seen in Fig. 7. In this figure, the x- and y- axes show the absolute position of the mobile station, thus it can directly be

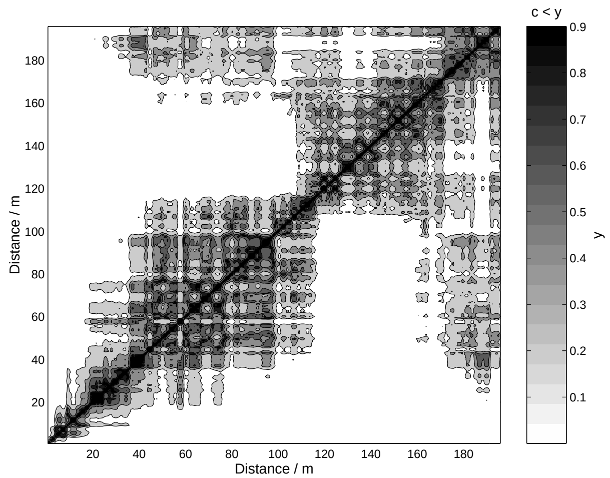

Fig. 5. Contour plot of the correlation coefficient c for Dresden-Prohlis.

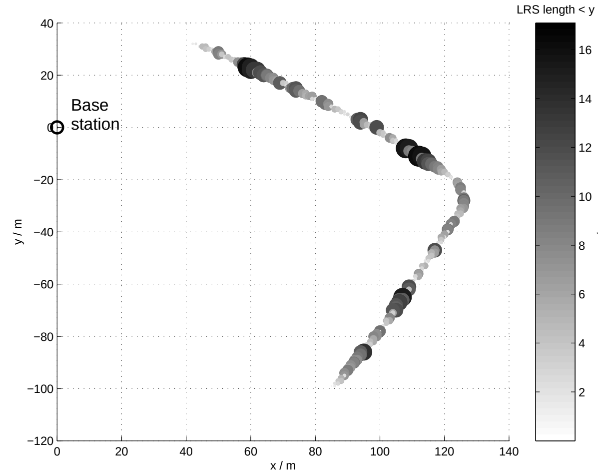

Fig. 7. Measured LRS lengths for Dresden-Prohlis.

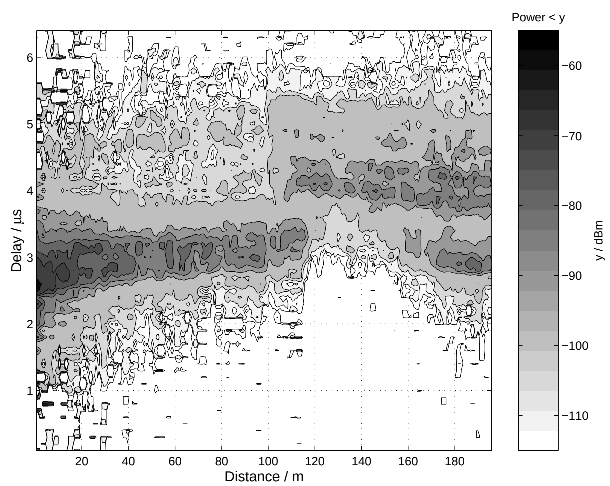

Fig. 6. Contour plot of the distance-dependent PDP for Dresden-Prohlis.

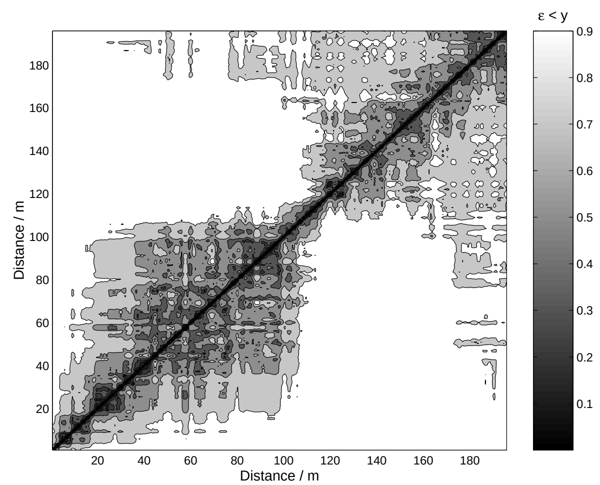

Fig. 8. Contour plot of the PDP error for Dresden-Prohlis.

compared to Fig. 3. The LRS assumes values of up to 20 meters when the irregularities along the mobile route are far away.

Up to now, the choice of correlation threshold was quite arbitrary. To ensure the error made by assuming a constant channel within the resulting LRS being low, we computed the relative PDP error ϵ, an evaluation of which is shown in Fig. 8. The error ϵ remains in the range $0.3 - 0.4$ for mobile positions within the stationarity region, while it exceeds 0.9 only little distances away on the outside. While 0.4 is not a negligible value, higher threshold values would lead to smaller LRS lengths and accordingly a higher number of separate channel segments. In the most extreme case, one LRS would comprise only a single channel snapshot which is of course most accurate but still does not help us for the simulation.

As can be expected, the LRS length depends on various parameters. To tackle this multiple dependencies, we envisaged a statistical approach. Data of approximately 15 to 20 measurement runs was processed to evaluate the cumulative distribution function (cdf) of LRS parameters for each environment.

Figure 9 shows the cdf of the LRS length for Dresden-Prohlis and Frankfurt station for different correlation coefficients. For a threshold value of 0.9, hardly any difference can be observed in the LRS lengths of different environments, while there is a clear deviation for values of 0.5 and 0.7. As a result, we suggest to use a threshold value of 0.5 where the different environments can clearly be separated.

Following this rule, Frankfurt exhibits significantly longer LRSs than Dresden. This is understandable from the completely different scattering scenario: The height of obstacles in Frankfurt (which are actually trains) is about 4 meters, while for Dresden (obstacles are surrounding buildings) their height is $\approx$ 20 meters. This has to be compared to the base station heights of 2.2m (Frankfurt) and 4.5m (Dresden)

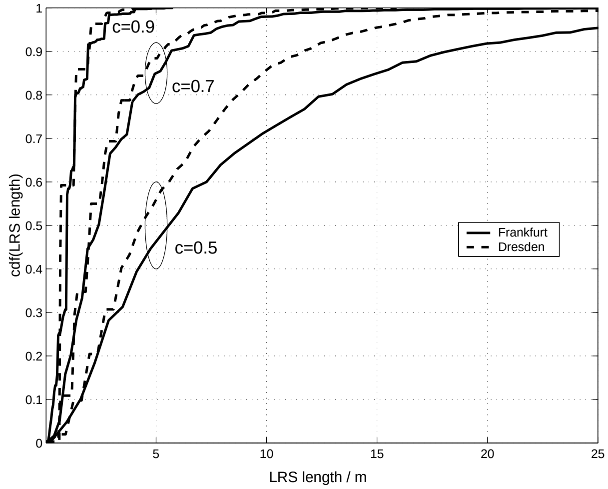

Fig. 9. Measured LRS lengths for Dresden-Prohlis and Frankfurt station for different correlation thresholds c.

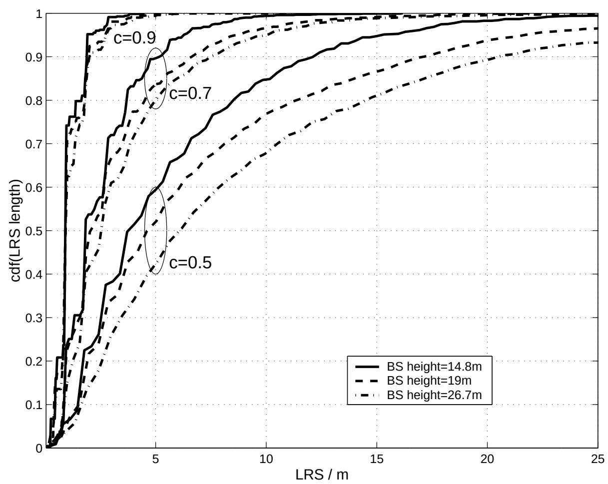

Fig. 10. Measured LRS lengths for Mannheim for different correlation thresholds c.

which in both cases is below the obstacles' heights but for Frankfurt the difference is much less (1.8m) than in Dresden (15.5m). To summarize, the LRS length increases the more macrocellular the scenario is while it reduces for the microcell case. These cell-types are used in the COST259 definition [9], where a macrocell has a base station antenna above rooftop while it is lowered below to give a microcell.

The LRS lengths for Mannheim are shown in Fig. 10 for different base station heights. It can be seen that the LRS increases with increasing height of the base station. The higher the base station (BS) is situated with respect to the surrounding obstructions, the less severe are the observed large-scale variations in the channel. Again, the LRS is positively correlated with the BS height.

To find a model for the large-scale correlation length of urban radio channels, we compared the

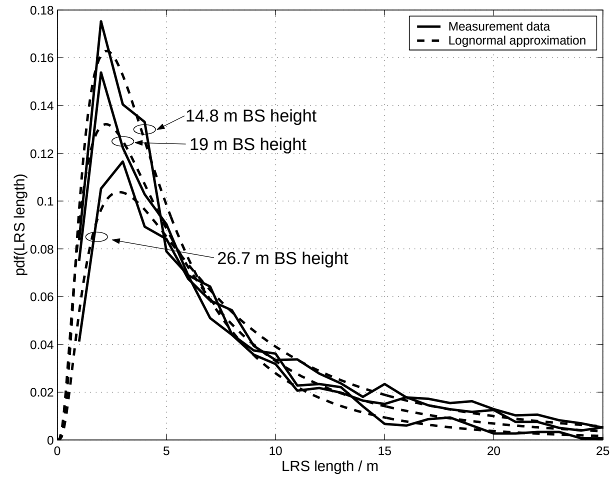

Fig. 11. PDF of the LRS lengths for Mannheim (solid) and the lognormal model (dashed) for different BS heights.

measurement data with common distribution functions. A good approximation for the LRS length was achieved by a lognormal distribution (see Fig. 11). A lognormal distribution is commonly assumed for the *fade-depth* through shadowing (see [1], Eq. (2-58)). Here, we found a similar model to apply for the *spatial length* of such fades. If we denote the LRS length by x, the probability density function $\mathrm{pdf}_x(x)$ can be written as

$$\mathrm{pdf}_x(x) = \frac{1}{\sqrt{2\pi\sigma_x^2}} \cdot \mathrm{e}^{-\frac{1}{2}\frac{(\ln x - \mu_x)^2}{\sigma_x^2}} \tag{8}$$

where μ_x and σ_x are the mean and standard deviation of x, respectively. The parameter values μ_x and σ_x to fit the measured pdf curves are listed in Tab. 1.

BS height-Building height	μ_x	σ_x
-15.5 m	1.5150	0.7486
-5.2 m	1.4421	0.7932
-1.8 m	1.7591	0.9043
-1 m	1.6145	0.9021
6.7 m	1.8564	0.9032

Tab. 1

Mean μ_x and standard deviation σ_x of the lognormal distribution of the LRS length (x).

A strong correlation between the difference between base station and building height and μ_x can be observed. The standard deviation on the other hand does not change severely for BS heights exceeding the average height of obstructions.

IV. Conclusions

We presented the concept of local stationarity regions of the mobile radio channel. The continuous stream of channel sounder measurement data was split into segments, each of which exhibits stationary behavior on a small-scale basis. The relative error between PDPs belonging to consecutive LRS segments depends on the threshold value of the correlation coefficient which is used to segment the data. For a value of $c_{th} = 0.5$, the relative error remains below 0.4 for a typical suburban environment thereby suggesting a reasonable segmentation on a cost/use basis. The lengths of extracted stationarity regions show a strong dependence on the investigated scenario, especially on the base station height and the average building height. Obtained measurement results for three typical environments were presented. The evaluated cdfs of the LRS lengths for different correlation coefficients motivate the use of the value 0.5 as a correlation threshold for the purpose of data segmentation. By a statistical analysis, we derived a lognormal model for the LRS length that can be used for large-scale channel simulations. The mean of the underlying lognormal distribution increases with the BS height relative to the average of surrounding obstructions' heights, but its variance is nearly height independent. The proposed segmentation procedure and the introduced large-scale parameter LRS length are deemed valuable means for both, evaluation of measurement results, and for determining the rate, amount and scaling of small-scale channel state transitions encountered by large-scale moving mobiles in a geometric simulation environment/equipment of scatterers.

Acknowledgements

Part of this work has been conducted within the EU-project METAMORP (Contract number SMT4-CT96-2093), under the program "Standards, Measurements and Testing" (SMT). We thank Prof. E. Bonek for his support and valuable suggestions.

Bibliography

[1] W.C.Y Lee, *Mobile Communications Engineering*, McGraw-Hill Book Company, New York, 1982.

[2] Theodore S. Rappaport, *Wireless Communications – Principles and Practice*, Number ISBN 0-7803-1167-1. IEEE Press, Prentice Hall PTR, 1996.

[3] P. A. Bello, "Characterization of randomly time-variant linear channels," *IEEE Trans. on Comm. Syst.*, vol. 11, pp. 360–393, Dec. 1963.

[4] Ralf Kattenbach, *Charakterisierung zeitvarianter Indoor-Funkkanäle anhand ihrer System- und Korrelationsfunktionen*, Ph.D. thesis, Universität-Gesamthochschule Kassel, 1997.

[5] R. Gollreither, "Channel Models Issue 2," Tech. Rep. R2084/ESG/CC3/DS/P/029/b1, RACE ATDMA, 1994.

[6] "Description of the modeling method," Tech. Rep., METAMORP – Public Report C-2/1, 1999.

[7] V. Perez and J. Jimenez, "Final Propagation Model," Tech. Rep. R2020/TDE/PS/DS/P/040/b1, RACE CODIT, 1994.

[8] Josef Fuhl, Andreas F. Molisch, and Ernst Bonek, "A unified channel model for mobile radio systems with smart antennas," in *IEE Proceedings on Radar, Sonar and Navigation; Special Issue on Antenna Array Processing Techniques*, Feb 1998, vol. 145, pp. 32–41.

[9] Luis Correia, Ed., *Wireless Flexible Personalized Communications – COST 259 Final Report*, John Wiley & Sons, Inc., to appear 2000.

[10] Robert J.C. Bultitude, G. Brussard, M.H.A.J. Herben, and T.J. Willink, "Radio channel modelling for terrestrial vehicular mobile applications," in *Proc. of the Millenium Conference on Antennas & Propagation (AP'2000)*, Davos, Switzerland, April 2000.